Chemical constituents

of the Arctic Ocean

in the Svalbard area

L. Anderson, D. Dyrssen
Department of Analytical and Marine Chemistry, Chalmers University of Technology and University of Göteborg, S-412 96 Göteborg, Sweden.

ABSTRACT

Data on the following constituents of the Eastern Arctic Ocean are treated: total alkalinity (A_t), total carbonate (C_t), calcium, nitrate, phosphate, silica and oxygen. The data were collected during the second part of the Swedish Arctic Expedition 1980 (Ymer 80). Mean values are given for the nutrient concentration at different depths. A revised silica budget for the Arctic Ocean is presented. The specific alkalinity (A_t/Cl) is higher in the outflowing East Greenland Current than in the inflowing West Spitsbergen Current. This is explained by an input of high alkalinity river water in the Transpolar Drift Stream. Chemical shifts in the surface water are explained by the formation of photosynthetic organic matter with the mean composition (stoichiometry) $(CH_2O)_{69}(NHCO)_{14}CHPO_4Mg(SiO_2)_7$. The oxygen concentrations are plotted against the *in situ* temperature and they correspond to a surface water saturated at $+3°$ in the Atlantic inflow. The deep undersaturation of carbon dioxide $(\leq 130$ ppm$)$ in the Arctic surface water around Svalbard can be explained by the photosynthetic uptake of carbon dioxide. This is demonstrated in a plot of $A_t - C_t$ against the *in situ* temperature. The intermediate and deep water data may be of special interest if the Atlantic Ocean water is formed in the Arctic.

Oceanol. Acta, 1981, **4**, 3, 305-311.

RÉSUMÉ

Composants chimiques de l'océan Arctique
dans la région de Svalbard

Des données sur les composants suivants de l'océan Arctique de l'Est ont été traitées : alcalinité (A_t), carbone inorganique total (C_t), calcium, nitrate, phosphates, silicates et oxygène dissous. Ces données avaient été recueillies en 1980, pendant la seconde partie de l'expédition suédoise Ymer 80 dans l'Arctique. Les valeurs moyennes de la concentration des sels nutritifs sont données à différentes profondeurs. Un nouveau bilan des silicates dans l'océan Arctique est présenté. L'alcalinité spécifique (A_t/Cl) est plus élevée dans le courant du Groenland sortant de l'océan Arctique à l'Est que dans le courant du Spitsberg qui y entre à l'Ouest. Ceci est expliqué par l'apport d'alcalinité dû aux eaux des rivières qui se produit dans le courant de dérive transpolaire. Les déviations de composition chimique qui existent dans l'eau de surface sont expliquées par la formation photosynthétique de matière organique de composition stœchiométrique moyenne $(CH_2O)_{69}(NHCO)_{14}CHPO_4Mg(SiO_2)_7$. Les concentrations en oxygène dissous ont été portées en fonction de la température potentielle; elles correspondent à l'eau de surface à $+3°C$ du courant qui entre dans l'Atlantique. La grande sous-saturation en gaz carbonique $(\leq 130$ ppm$)$ de l'eau de surface de l'océan Arctique autour de Svalbard peut être expliquée par la consommation photosynthétique de gaz carbonique. Ceci est

démontré sur un graphique où $A_t - C_t$ est porté en fonction de la température potentielle. Les données sur les eaux intermédiaires et profondes peuvent être d'un grand intérêt si l'eau de l'océan Atlantique est formée dans l'Arctique.

Oceanol. Acta, 1981, **4**, 3, 305-311.

INTRODUCTION

Leg 2 of the Swedish Arctic expedition (Ymer 80) from August 10 to September 24, 1980 provided us with the opportunity to determine some constituents of the Arctic Ocean in the Svalbard area. The following constituents will be treated in this paper: total alkalinity (A_t), total carbonate (C_t), calcium, nitrate, phosphate, silica and oxygen. The same concentration scale (μmol/kg seawater, $μM_w$) will be used as in the Geosecs program. The concentrations together with positions, depths, temperatures and salinities are available in a data report (Anderson, Dyrssen, 1980). The CTD data will be published and treated separately by Rudels and Sehlstedt at the Department of Oceanography, University of Göteborg. Data on Leg 1 of the Ymer 80 expedition (N and NE of Svalbard on July 4-August 5, 1980) will be published separately by Dahlin and Valderrama at the Fishery Board of Sweden. The positions of the sampling stations are shown in Figure 1.
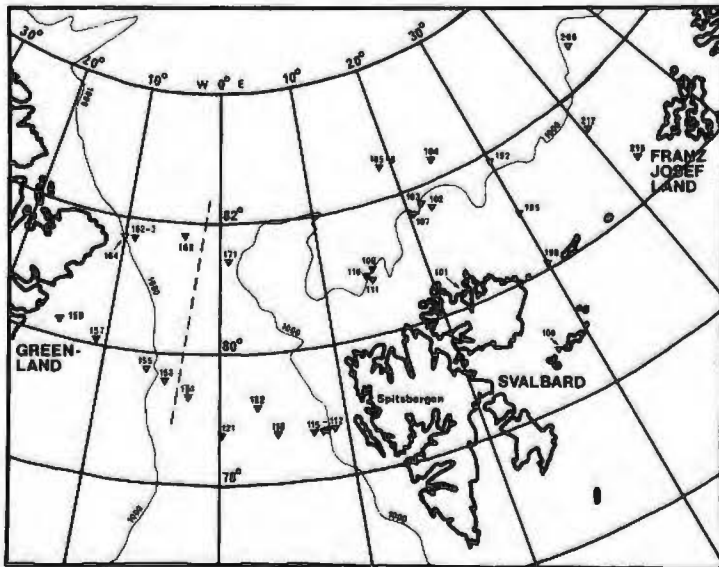

Figure 1
Station locations of Leg 2 of the Ymer 80 expedition.

METHODS

The sampling was carried out with a single Rosette sampler with twelve 2.5 l. Niskin bottles attached to the CTD probe (Neil Brown). Occasionally, 1.7 l. Hydrobios samplers were used. Surface water (7 m) samplers were drawn from an intake in the ship's hull. The Swedish icebreaker Ymer was provided with satellite navigation, and positions were obtained from the bridge.
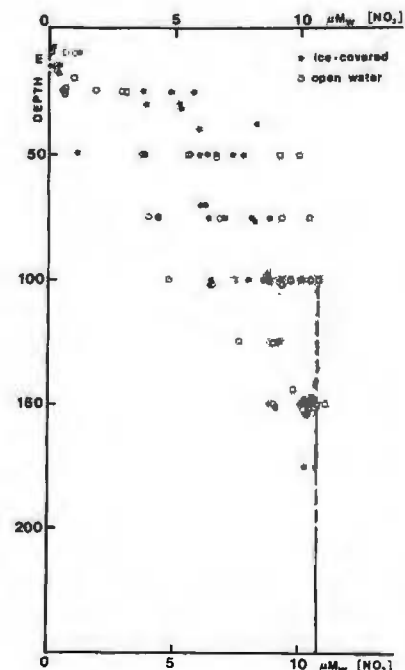
The total alkalinity was determined by a computerized photometric titration with hydrochloric acid. The method used was a modification of the method published by Granéli and Anfält (1977). The pH of each water sample was determined at the temperature in the container laboratory according to Almgren *et al.* (1975), and C_t was calculated from A_t, pH, buffer temperature and salinity. Calcium was determined by a photometric EGTA titration (Jagner, 1974). The method was computerized and adapted to on board work, using 10 ml of sample per analysis (Anderson, Granéli, 1981). The nutrients and oxygen were determined according to the New Baltic Manual (Carlberg, 1972) except that the oxygen concentration (μmol/kg seawater) was calculated from $vt \times 10^6/4$ (V-1) 1.025 where v is the volume (ml) and t the titre of the thiosulfate solution (0.020 02 N) and V the volume (ml) of the Winkler bottle.

NUTRIENT LEVELS

Table 1 demonstrates that the levels of nitrate and phosphate at the depths of 200 to 500 m did not vary from 15°W to 45°E during July, August and September. Table 2 shows that the mean values for nitrate (10.74 $μM_w$) and phosphate (0.79 $μM_w$) for 200-500 m

Figure 2
Depth profile of the nitrate concentrations in surface Arctic seawater. The mean value of 200-500 m is indicated with a vertical line at 10.74 $μM_w$.

Table 1

Overview of the concentrations of nitrate, phosphate and silica of the Arctic Ocean in the Svalbard area. The number of analyses given in parenthesis.

	Latitude 80°16′N Longitude 15°14′W Station No. 159	79°34′N-81°43′N 10°58′W-3°31′W 153, 162, 164, 168	79°21′N-81°24′N 2°31′W-0°52′E 151, 171	78°45′N-81°00′N 0°02′E-14°57′E 109, 110, 115, 121 122	81°35′N-82°30′N 18°41′E-29°47′E 102, 103, 104, 105, 192	82°19′N-82°29′N 38°24′E-38°37′E 25, 26	82°23′N-82°28′N 44°40′E-45°08′E 23, 24, 206
Depth: 200-500 m:							
N	11.2(2)	10.91(14)	10.78(8)	10.82(17)	10.85(13)	10.28(4)	10.29(10)
P	0.85(2)	0.782(13)	0.748(8)	0.814(17)	0.795(13)	0.793(4)	0.779(10)
Si	9.64(2)	6.14(14)	5.34(8)	5.42(17)	5.28(13)	5.39(4)	5.25(9)
Depth:							
≧ 750 m N		11.91(17)	12.54(7)	12.80(22)	12.68(25)	12.05(5)	11.86(7)
≧ 750 m P		0.875(17)	0.879(7)	0.940(22)	0.905(25)	0.954(5)	0.900(7)
750-800 m Si		6.77(4)	7.71(1)	7.58(2)	7.47(3)	–	7.47(3)
1 000 m Si		7.25(4)	8.29(2)	8.55(4)	8.54(6)	9.30(1)	9.10(2)
> 1 000 m Si		9.30(8)	10.31(4)	10.57(16)	10.31(16)	10.72(4)	10.59(2)

Table 2

Mean values of some constituents of the Arctic Ocean in the Svalbard area.

Constituent	Concentrations (μM_w) at depths			
	200-500 m	750-800 m	1 000 m	> 1 000 m
Nitrate	10.74	12.44	12.44	12.44
Phosphate	0.79	0.91	0.91	0.91
Silica	5.34	7.29	8.34	10.28
Alkalinity	2 330	2 331	2 331	2 331
Total carbonate	2 171	2 185	2 185	2 185
$A_t - C_t$	159	146	146	146
Oxygen	318 (305*)	309	309	309

(*) East Greenland waters.

were slightly lower than the concentrations at depths below 500 m, 12.44 and 0.91 μM_w respectively. The ratios nitrate to phosphate were close to 14 (13.6 and 13.7 for the intermediate and deep water). Above 150 m the nutrient concentrations varied considerably with depth as shown for nitrate in Figure 2. The surface water concentrations were low down to 20 m and scatter from 25 to 100 m. Ice-covering could hamper the photosynthetic uptake of nitrate, but this is only discernible in Figure 2 at 25 to 40 m.
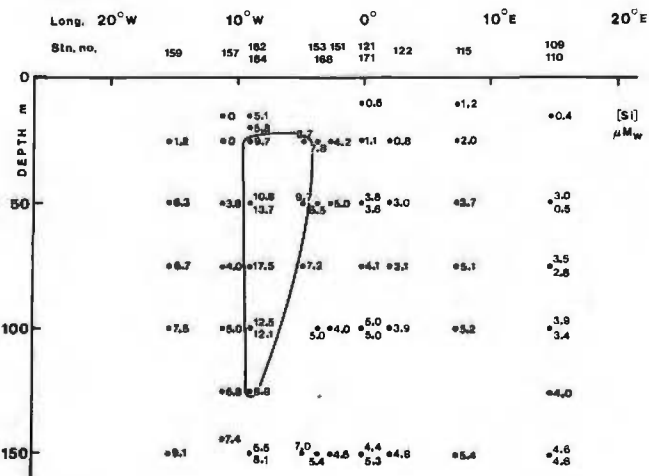
Figure 3

Silica concentrations between Greenland and Svalbard close to 80°N (station locations are given in Fig. 1).

The silica concentrations increased all the way down to the deep water below 1 000 m as shown by Table 1. The values for the deep water agree with those found by Moore and Lowings (1981) for the Fram Basin. The nitrate/silica ratio decreased from 2 to 1.2. In his papers on the silica budget for the Arctic Ocean, Codispoti (see Codispoti, Owens, 1975) used 8 μM for the concentration of silica in the Transpolar-East Greenland Drift Stream and 5 μM for the inflowing Atlantic Water and Arctic Bottom Water. Table 1 demonstrates that the silica concentration increased from 5.35 to 6.14 μM_w at 200-500 m as we passed the front (dashed line in Fig. 1). Close to Greenland the concentration increased to 9.64 μM_w. The situation between Svalbard and Greenland for the surface water above 200 m is shown in Figure 3. A core of high silica water appears between 25 and 125 m in the East Greenland Current. This can be a reminiscence of the silica maximum at 55 to 130 m (with 15 to 36 μM) observed close to the North Pole by Moore and Lowings (1981).

A silica budget for the Arctic Ocean is shown in Table 3.

Table 3

A silica budget for the Arctic Ocean

	Volume [a] (m^3/sec.)	Silica conc. (μM)	Silica transport (kmol/sec.)
Inflows:			
Atlantic water	$7.8 \cdot 10^6$	5	+ 39.0
Bering strait	$1.5 \cdot 10^6$	35	+ 52.5
Runoff	$0.1 \cdot 10^6$	125 [b]	+ 12.5
	$9.4 \cdot 10^6$		+104.0
Outflows:			
Atlantic water	$5.4 \cdot 10^6$	5	− 27.0
Polar water	$1.8 \cdot 10^6$	15 [c]	− 27.0
Sea ice	$0.1 \cdot 10^6$	5 ?	− 0.5
Canadian Archipelago	$2.1 \cdot 10^6$	21 [d]	− 44.1
	$9.4 \cdot 10^6$		− 98.6

[a] from Aagaard and Greisman (1975).
[b] from Codispoti and Owens (1975).
[c] the mean concentration of silica in the East Greenland outflow (Atlantic + polar water) is about 7.5 μM, which is based on our data in Figure 3. This gives a value of about 15 μM for the polar water.
[d] from Jones and Coote (1980).

This budget is slightly different from the budget of Codispoti and Owens (1975), which has been revised by Jones and Coote (1980). Volume transports were taken from Aagaard and Greisman (1975). A treatment of the silica data below indicates that the silica in the river water is removed by biological processes (cf. Aston, 1980). Such a removal is also indicated by the budget deficit of 5.4 kmol/sec. in Table 3. The budget shows that silica from the Pacific Ocean is transferred to the Atlantic Ocean through the Arctic Ocean.

The Arctic Ocean deep water, which may be formed in the Greenland Sea, can be regarded as a source water for the deeper Norwegian Sea and North Atlantic Ocean. Table 2 gives the mean values for the deep water between Greenland and Svalbard (stations 102-171). The increase of nitrate and phosphate below 500 m is most likely due to oxidation of organic matter. This is also reflected in the increase in total carbonate. The increase of silica with depth (Table 2) is of course due to the sinking and dissolution of biogenic opal. The constant alkalinity and specific alkalinity ($A_t/Cl = 0.1207$ mM$_w$/^{o}/$_{oo}$) shows the biogenic production of calcium carbonate with the corresponding sinking and dissolution of calcium carbonate shells is of no importance in the Arctic Ocean in contrast with the Pacific Ocean (see Almgren et al., 1977). This is also reflected in the constant Ca/Cl (0.5299 mM$_w$/$\%_{oo}$ as compared with 0.5306 for standard seawater).

THE FRONT

The front between the Atlantic inflowing water and Transpolar-Greenland Drift Stream (dashed line in Fig. 1) can be seen from the data from stations 151 (79°21'N, 2°31'W) and 153 (79°34'N, 4°43'W) as well as stations 171 (81°24'N, 0°52'E) and 168 (81°43'N, 3°31'W). In Figure 4 the salinities show the front down to
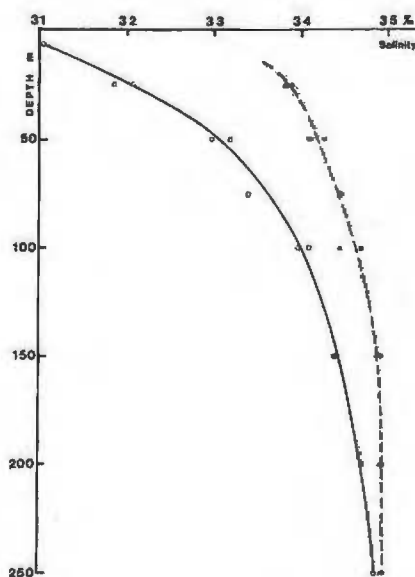

Figure 5
Surface water values of the specific alkalinity at the front. For notations see Figure 4.

250 m and in Figure 5 the specific alkalinities show that the low salinity Greenland current water has higher A_t/Cl. This will be treated in the next section.

RIVER INPUTS

Approximately 0.23×10^6 ton ice is annually accumulated in the Arctic Ocean (Koerner, 1973). A balance is achieved by ice export (about 50%) and ablation (about 50%). Melting should lower the salinity of the surface seawater in the period June to September. Input of river water (approximately 0.1×10^6 m^3/sec.; see Aagaard, Greisman, 1975) should have the same effect. Melting and freezing of sea ice would change the specific alkalinity (A_t/Cl) and the concentration of calcium if calcium carbonate is precipitated on the brine channel walls when sea ice is formed (Jones et al., 1981). Thus the increase in A_t/Cl shown in Figure 5 could be due to melt water or an inflow of high alkalinity river water. However, analysis of water sampled at the 1979 Lorex drift station at the North Pole by the oxygen isotope technique showed no input of melt water (Francis Tan, pers. comm.; see Tan,

Figure 4
Surface water salinities on both sides of the front between the Atlantic water inflow and the Greenland current outflow. Stations: ●, 151; ▲, 171; ○, 153; □, 168 (see Fig. 1).
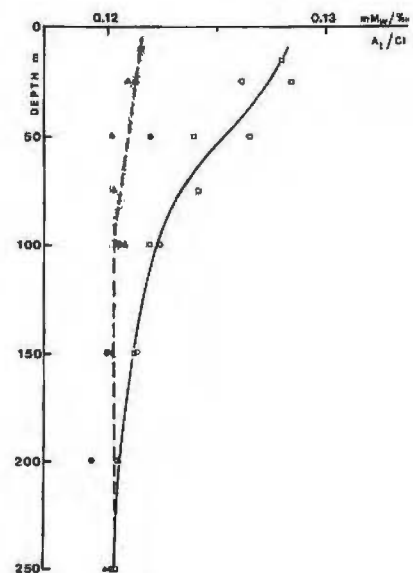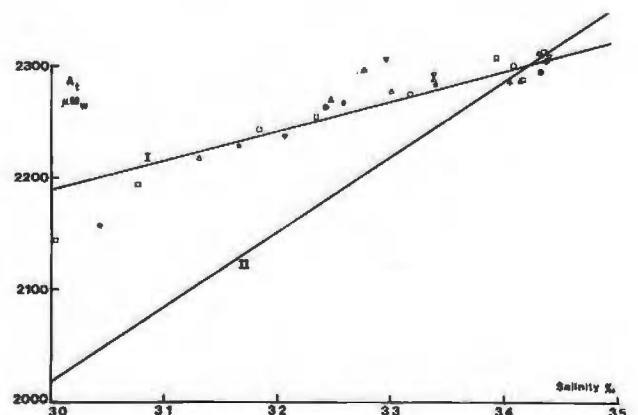

Figure 6
Alkalinity versus the salinity of East Greenland current surface water (≤ 150 m). Stations: ▽, 153; △, 157; ●, 159; □, 163; ★, 164; ○, 168.

Strain, 1980 and Moore, Lowings, 1981). Transport by the Beaufort Gyral Stream and Transpolar Drift Stream could carry water from the Mackenzie, Kolyma, Indigirka, Lena and Yana rivers into the East Greenland Current.

In Figure 6 we have plotted the alkalinity against the salinity. The line I with $A_t = 26.33 \ S + 1\ 400 \ \mu M_w$ fits the data, while the equation $A_t = 67.24 \ S$ (line II) with zero residual alkalinity does not fit. This implies an input of melt water containing calcium carbonate, which has been dissolved

$$CaCO_3 (s) + CO_2 + H_2O \rightarrow Ca^{2+} + 2\,HCO_3^-,$$
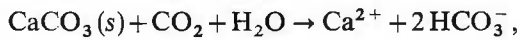
or an input of high alkalinity river water with $A_t = 1\ 400 \ \mu M_w$ (see Anderson, Dyrssen, 1981 and Dyrssen, Wedborg, 1980 a). Since the alkalinity input mainly consists of $Ca(HCO_3)_2$ an equation with a residual calcium concentration of $700 \ \mu M_w$ or $0.7\,mM_w$ should fit the corresponding calcium data. In Figure 7 we have drawn the line with the equation $Ca_t = 0.2723 \ S + 0.7\,mM_w$. This line fits the data quite well.
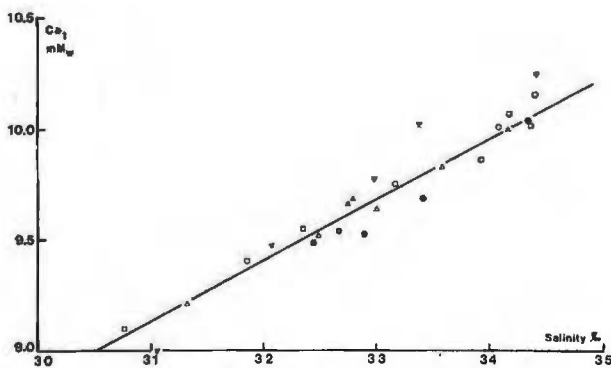

Figure 7
Calcium concentration against salinity of East Greenland current surface water ($\leq 150 \ m$). Station notations as in Figure 6.

In Figure 8 we plotted the silica concentrations against the salinities. Line I with the equation $[SiO_2] = -3.34 \ S + 125 \ \mu M_w$ is drawn with the residual silica of $125 \ \mu M$ according to Codispoti and Owens (1975). We have also drawn the line with zero river water silica. This line has the equation $[SiO_2] = 0.316 \ S \ \mu M_w$. In doing so, however, we have corrected the low silica values for bioproduction using silica-phosphate data from surface waters at stations 109, 110, 115, 121 and 122.

We therefore conclude that the melt water or river water does not supply very much silica. This would imply that silica is not precipitated in sea ice or that the production of biogenic opal and settling processes remove the silica brought into the Arctic Ocean by the rivers (cf. Aston, 1980). Oxygen isotope techniques could establish the proportion of melt water in the summer water of the East Greenland current (cf. Tan, Strain, 1980). Water samples will be sent to Dr. Francis Tan for oxygen isotope determinations.
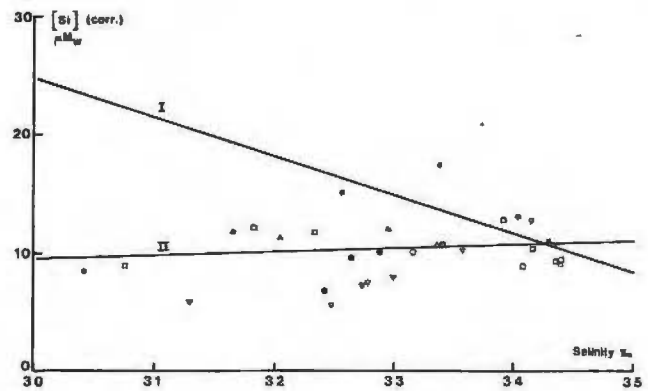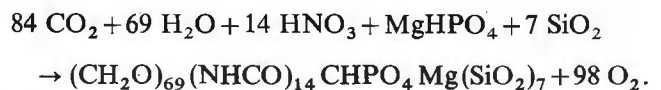

Figure 8
Concentration of silica versus salinity of East Greenland current surface water ($\leq 150 \ m$). Station notations as in Figure 6.

THE OXYGEN LEVELS

Our data show considerable supersaturation of oxygen in the top 25 to 50 m. In order to correct for the photosynthetic production of oxygen we need a chemical model for the photosynthetic matter. Following the Redfield model modified by Dyrssen (1977) we plotted $C_t 35/S$ (total carbonate normalized to 35 ‰ salinity) and $[NO_3] 35/S$ for surface waters at stations 102, 103, 104, 105, 109, 110, 115, 121, 122, 151 and 171. This gave us a $C_t/[NO_3^-]$ ratio close to 6. The nitrate/phosphate ratio was close to 14 and the nitrate/silica ratio of the water at 200-500 m was close to 2. Thus the model substance for the Arctic Ocean in Svalbard area would have the $C : N : P : Si$ ratio $84 : 14 : 1 : 7$. The production takes place by the following reaction:

$$84 \ CO_2 + 69 \ H_2O + 14 \ HNO_3 + MgHPO_4 + 7 \ SiO_2$$

$$\rightarrow (CH_2O)_{69} (NHCO)_{14} CHPO_4 Mg(SiO_2)_7 + 98 \ O_2.$$

The chemical shifts are:

$\Delta C_t = -84,$

$\Delta NO_3 = -14,$

$\Delta PO_4 = -1,$

$\Delta O_2 = +98,$

$\Delta A_t = +13.$

The production of photosynthetic matter should therefore lead to the following corrections assuming the nitrate concentration is close to $11 \ \mu M_w$ (see Fig. 2):

$$C_t(corr) = \frac{84}{14}(11 - [NO_3]),$$

$$A_t(corr) = -\frac{13}{14}(11 - [NO_3]),$$

$$(A_t - C_t)(corr) = -\frac{97}{14}(11 - [NO_3]),$$

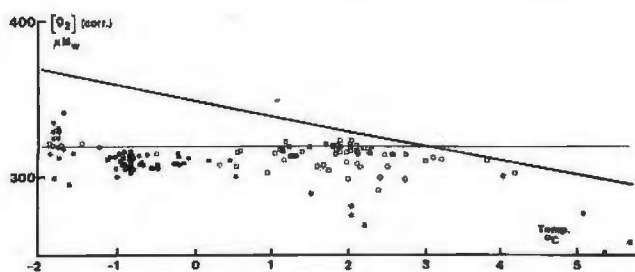$$O_2(corr) = -\frac{98}{14}(11 - [NO_3]).$$

Figure 9

Oxygen concentrations of Atlantic inflowing waters versus the in situ water temperature. Stations: 102, 103, 104, 105, 109, 110, 115, 121, 122, 151 and 171. Depths: ★, ≤ 50 m; ○, 50-150 m; □, > 150-500 m; ●, > 500 m. The straight line represents saturation with air at a pressure of 760 mm Hg. The thin line corresponds to 320 μM_w and saturation at 3°.
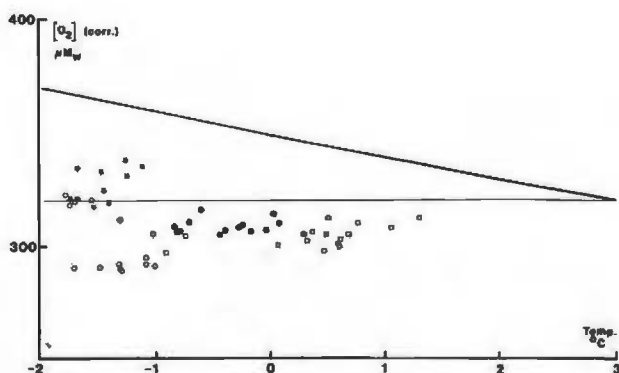

Figure 10

Oxygen concentrations of the East Greenland current water as a function of the in situ water temperature. Stations: 153, 157, 162-163, 164 and 168. Depth notations as in Figure 9.

Using this correction for oxygen for the waters above 150 m we arrive at the plots in Figures 9 and 10. In these figures the saturation level is drawn as a function of the temperature. Some relatively warm surface waters seem to have been overcorrected which implies that some of the photosynthetically produced oxygen has escaped into the atmosphere. Apart from this all waters were undersaturated or correspond to a surface water of about +3° which has been cooled off with subsequent sinking. The following mean oxygen values have been calculated from uncorrected data:

	150-500 m	> 500 m
Atlantic inflow	318.3 μM_w	309.5 μM_w
East Greenland outflow	304.7 μM_w	307.3 μM_w

The higher value of the inflowing Atlantic Ocean water from the Norwegian Sea may be an effect of photosynthesis in the surface water. The production in the Transpolar-Greenland Drift Streams is probably small. The average value for the deep water (> 500 m) was close to 309 μM_w. If the Arctic Ocean and Greenland Sea deep water should be regarded as a source water for the Atlantic Ocean then the so-called performed concentrations of the constituents are those given in Table 2.

THE CARBON DIOXIDE UNDERSATURATION

Investigations by Kelley (1970) of the Kara and Barents Seas during the late summer of 1967 show undersaturation. We find this undersaturation from a plot of $A_t - C_t$ against the temperature for surface waters down to 50 m and occasionally down to 100 m. This concurs with separate measurements by Gosink during the Ymer 80 expedition. Since carbon dioxide is consumed for the production of phytoplankton we corrected the surface waters down to 150 m with the formula derived above:

$$(A_t - C_t)(corr) = -7(11 - [NO_3]) μM_w.$$

Since some surface waters have very low nitrate concentrations the correction can be as large as 75 μM_w which corresponds to about 130 ppm CO_2 [$Δ(A_t - C_t)/Δp_{CO_2} \simeq 0.6$ μM_w/ppm; see Dyrssen, Wedborg, 1980 b]. The corrected values of $A_t - C_t$ are plotted against the *in situ* temperature of the water sample in Figure 11. The data fall close to a line calculated by Dyrssen and Wedborg (1980 b) for 330 ppm CO_2 in the atmosphere. This is about 4 ppm lower than the present value for the northern atmosphere that can be estimated from Machta *et al.* (1977). The data seem on the whole to have a smaller temperature slope than can be calculated from equilibrium constants. This can be explained by ice cooling of surface water of about 0° and summer heating of warmer surface waters (about 3 to 5°) in which case equilibrium has not yet been established. Since $A_t - C_t$ will only decrease about 6 μM_w for an increase of the partial pressure of CO_2 of 10 ppm, the scatter of the data in Figure 11 correspond to an uncertainty of ± 15 ppm CO_2. This scatter is partly due to the error of the determinations of the alkalinity and total carbonate and partly due to the patchiness of the plankton production (Lars Edler, pers. comm.). One conclusion that may be drawn from the deep water data (> 500 m) is that they may be formed by rather rapid vertical mixing processes. A preindustrial dashed line for 280 ppm CO_2 is shown in Figure 11. Obviously, the deep Arctic Ocean water does not seem to be very old. This is in contrast to
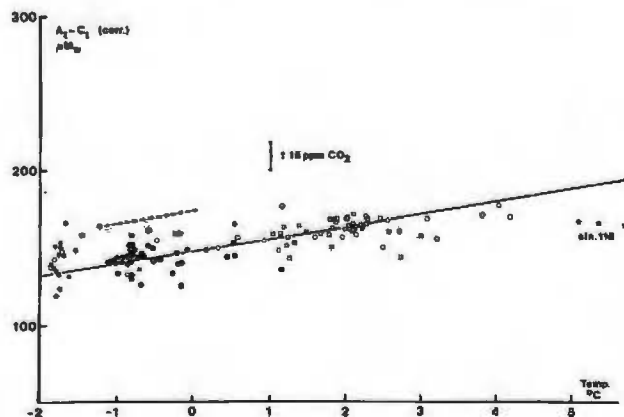

Figure 11

Alkalinity-total carbonate corrected for photosynthetic consumption of carbon dioxide as a function of the in situ water temperature of the sample. Stations and notations as in Figure 9. The straight line represents saturation with 330 ppm carbon dioxide in the air; the dashed line 280 ppm.

the low oxygen deep water in Baffin Bay (Jones, Levy, 1981). Further information on the vertical mixing of the Arctic Ocean will be obtained when the samples for tritium and carbon-14 determinations have been analyzed. The work presented in this section will be compared with the direct gaschromatographic determinations of CO_2 in air and surface water carried out by Dr. Thomas Gosink.

FUTURE WORK

Since most of the constituents determined in this work seem to be dependent on photosynthesis and the temperature of the surface water, comparative investigations should be carried out in January-March. Furthermore, a special cruise should be devoted to study the inputs of the large rivers (Mackenzie, Kolyma, Lena, Yenisey and Ob). This calls for a joint venture with Canadian and Soviet scientists. Together with University of Alaska the constituents of the Bering and Chukchi Seas could be measured in order to determine the impact of the Pacific Water on the Arctic Ocean. The influence of the formation of sea ice and melt water on the alkalinity and total carbonate should be further investigated. Since several water masses are mixed in the Arctic Ocean the straight lines in Figures 6-8 might be replaced by two or three mixing lines in a more detailed treatment.

REFERENCES

Aagaard K., Greisman P., 1975. Toward new mass and heat budgets for the Arctic Ocean, *J. Geophys. Res.*, **80**, 3821-3827.

Almgren T., Dyrssen D., Strandberg M., 1975. Determination of pH on the moles per kg seawater scale (M_w), *Deep-Sea Res.*, **22**, 635-646.

Almgren T., Dyrssen D., Strandberg M., 1977. Computerized high-precision titrations of some major constituents of seawater on board the R.V. Dmitry Mendeleev, *Deep-Sea Res.*, **24**, 345-364.

Anderson L., Dyrssen D., 1980. *Constituent data for Leg 2 of the Ymer 80 expedition*, Report on the Chemistry of Seawater XXIV, Department of Analytical and Marine Chemistry, Göteborg, Sweden.

Anderson L., Dyrssen D., 1981. Excess calcium and alkalinity in the Baltic and Southern Kattegatt, *Oceanol. Acta*, **4**, 1, 3-6.

Anderson L., Granéli A., 1981. *A compact automated titration system applied to a high precision determination of calcium in sea water*, to be published.

Aston S. R., 1980. Nutrients, dissolved gases, and general biogeochemistry in estuaries. Chapt. 7, in: *Chemistry and biogeochemistry of estuaries*, edited by E. Olausson and I. Cato, John Wiley.

Carlberg S. R., 1972. New Baltic manual, *ICES Coop. Res. Rep.*, Ser. A, **29**.

Codispoti L. A., Owens T. G., 1975. Nutrient transports through Lancaster Sound in relation to the Arctic Ocean's reactive silicate budget and the outflow of Bering Strait waters, *Limnol. Oceanogr.*, **20**, 115-119.

Dyrssen D., 1977. The chemistry of plankton production and decomposition in seawater, in: Oceanic sound scattering prediction, edited by N. R. Andersen and B. J. Zahuranec, *Mar. Sci.*, **5**, Plenum Press.

Dyrssen D., Wedborg M., 1980 a. Major and minor elements, chemical speciation in estuarine waters. Chapt. 3, in: *Chemistry and biogeochemistry of estuaries*, edited by E. Olausson and I. Cato, John Wiley.

Dyrssen D., Wedborg M., 1980 b. The influence of the partial pressure of carbon dioxide on the total carbonate of seawater, submitted to *Mar. Chem.*

Granéli A., Anfält T., 1977. A simple automatic phototitrator for the determination of total carbonate and total alkalinity of sea water, *Anal. Chim. Acta*, **91**, 175-180.

Jagner D., 1974. High-precision determination of calcium in the presence of higher concentration of magnesium by means of a computerized photometric titration, *Anal. Chim. Acta*, **68**, 83-92.

Jones E. P., Coote A. R., 1980. Nutrient distributions in the Canadian Archipelago: indicators of summer water mass and flow characteristics. *Can. J. Fish. Aqu. Sci.*, **37**, 589-599.

Jones E. P., Levy E. M., 1981. Oceanic CO_2 increase in the Baffin Bay, submitted to *J. Mar. Res.*

Jones E. P., Coote A. R., Levy E. M., 1981. Effect of sea ice meltwater on the alkalinity of seawater, submitted to *J. Geophys. Res.*

Kelley J. J., 1970. Carbon dioxide in the surface waters of the North Atlantic Ocean and the Barents and Kara Seas, *Limnol. Oceanogr.*, **15**, 80-87.

Koerner R. M., 1973. The mass balance of the sea ice of the Arctic Ocean, *J. Glaciol.*, **12**, 173-185.

Machta L., Hanson K., Keeling C. D., 1977. Atmospheric carbon dioxide and some interpretations, in: *The fate of fossil fuel CO_2 in the oceans*, edited by N. R. Andersen and A. Malahoff, *Mar. Sci.*, **6**, Plenum Press.

Moore R. M., Lowings M. G., 1981. Hydrographic features and nutrients at the Lorex station in the central Arctic Ocean, submitted to *Gochim. Cosmochim. Acta.*

Tan F. C., Strain P. M., 1980. The distribution of sea ice meltwater in the Eastern Canadian Arctic, *J. Geophys. Res.*, **85**, 1925-1932.

Actes du Congrès de Géologie/*Proceedings of the Geological Congress*

COLLOQUE C₃

Géologie des marges continentales/*Geology of continental margins*

O. Eldholm, L. Montadert, *The main types of passive margins: an introduction.*

J. A. Grow, R. E. Sheridan, *Structure and evolution of the US Atlantic continental margin.*

K. Hinz, H. Dostmann, J. Fritsch, *The continental margin of Morocco: seismic sequences, structural elements and the geological development.*

M. Talwani, J. Mutter, O. Eldholm, *The initiation of opening of the Norwegian Sea.*

J. Hardenbol, P. R. Vail, J. Ferrer, *Interpreting paleoenvironments, subsidence history and sea-level changes of passive margins from seismic and biostratigraphy.*

J. S. Schlee, L. F. Jansa, *The paleoenvironment and development of the eastern North-American continental margin.*

T. S. Loutit, J. P. Kennett, *Australasian Cenozoic sedimentary cycles, global sea level changes and the deep-sea sedimentary record.*

J. Thiede, *Late Mesozoic and Cenozoic sedimentation along oceanic island margins: analog to continental margins.*

S. W. Petters, *Paleoenvironments of the Gulf of Guinea.*

A. W. Bally, D. Bernoulli, G. A. Davis, L. Montadert, *Listric normal faults.*

D. A. Falvey, M. F. Middleton, *Passive continental margins: evidence for a prebreakup deep crustal metamorphic subsidence mechanism.*

R. Meissner, *Passive margin development. A consequence of specific convection patterns in a variable viscosity upper mantle.*

C. E. Keen, C. Beaumont, R. Boutilier, *Preliminary results from a thermo-mechanical model for the evolution of Atlantic-type continental margins.*

R. T. Buffler, F. J. Shaub, R. Huerta, A. B. Ibrahim, J. S. Watkins, *A model for the early evolution of the Gulf of Mexico Basin.*

J. C. Crowell, *Juncture of San Andreas transform system and Gulf of California rift.*

A. B. Watts, M. S. Steckler, *Subsidence and tectonics of Atlantic-type continental margins.*

J. R. Cochran, *Simple models of diffuse extension and the pre-seafloor spreading development of the continental margin of the Northeastern Gulf of Aden.*

E. V. Artyushkov, *Physical origin of crustal movements on passive margins.*

R. von Huene, *Introduction to papers presented at the Geology of continental margins symposium (active margins section), International Geological Congress, Paris 1980.*

M. G. Langseth, R. von Huene, N. Nasu, H. Okada, *Subsidence of the Japan Trench forearc region of Northern Honshu.*

G. deV. Klein, K. Kobayashi, *Geological summary of the Shikoku Basin and northwestern Philippine Sea, Leg 58, DSDP/IPOD drilling results.*

J. S. Watkins, J. C. Moore, T. H. Shipley, S. B. Bachman, F. W. Beghtel, A. Butt, B. M. Didyk, J. K. Leggett, N. Lundberg, K. J. McMillen, N. Niitsuma, L. E. Shepherd, J. F. Stephan, H. Stradner, *Accretion, underplating, subduction and tectonic evolution Middle America Trench, Southern Mexico: results from DSDP Leg 66.*

Y. Ida, *Thermal circulation of partial melt and volcanism behind trenches.*

E. V. Artyushkov, *Mechanism of formation of active margins.*

E. Honza, *Subduction and accretion in the Japan Trench.*

R. C. Speed, *Geology of Barbados: implications for an accretionary origin.*

M. C. Blake Jr., A. S. Jayko, D. G. Howell, *Geology of a subduction complex in the Franciscan assemblage of Northern California.*

X. Le Pichon, P. Huchon, J. Angelier, N. Lybéris, J. Boulin, D. Bureau, J.-P. Cadet, J. Dercourt, G. Glaçon, H. Got, D. Karig, J. Mascle, L.-E. Ricou, F. Thiébault, *Active tectonics in the Hellenic Trench.*

J. Aubouin, R. Blanchet, *Subduction and tectonics: discussion on the results of the IPOD program in active margins.*

J. Aubouin, R. von Huene, J. Azema, G. Blackinton, J. A. Carter, W. T. Coulbourn, D. S. Cowan, J. A. Curiale, C. A. Dengo, R. W. Faas, W. Harrison, R. Hesse, D. M. Hussong, J. W. Ladd, N. Muzylov, T. Shiki, P. R. Thompson, J. Westberg, *A summary of Deep Sea Drilling Project Leg 67. Shipboard results from the Mid-America Trench transect off Guatemala.*

R. B. Scott, L. Kroenke, *Periodicity of remnant arcs and back-arc basins of the South Philippine Sea.*

R. von Huene, S. Uyeda, *A summary of results from the IPOD transects across the Japan, Mariana, and Middle-America convergent margins.*

D. M. Hussong, S. Uyeda, *Tectonics in the Mariana arc: results of recent studies, including DSDP Leg 60.*

COLLOQUE C₄

Géologie des océans/*Geology of oceans*

R. C. Searle, A. S. Laughton, *Fine-scale sonar study of tectonics and volcanism on the Reykjanes Ridge.*

C. Rangin, J. Francheteau, *Fine scale morphological and structural analysis of the East Pacific Rise, 21°N (Rita project).*

C. R. B. Lister, *Rock and water histories during sub-oceanic hydrothermal events.*

D. S. Cronan, S. P. Varnavas, *Hydrothermal and dissolution related geochemical variations in sediments from an East Pacific Rise fracture zone at 9°S.*

J. B. Corliss, J. A. Baross, S. E. Hoffman, *Submarine hydrothermal systems: a probable site for the origin of life.*

B. U. Haq, *Paleogene paleoceanography: Early Cenozoic oceans revisited.*

M. A. Arthur, H. C. Jenkyns, *Phosphorites and paleoceanography.*

B. Tissot, R. Pelet, *Sources and fate of organic matter in ocean sediments.*

M. Steinberg, *Biosiliceous sedimentation, radiolarite periods and silica budget fluctuations.*

H. Chamley, *Long-term trends in clay deposition in the ocean.*

J. M. Gieskes, J. R. Lawrence, *Geochemical significance of diagenetic reactions in ocean sediments: an evaluation of interstitial water data.*

K. J. Hsü, *Origin of geochemical anomaly at Cretaceous-Tertiary boundary. Asteroid or cometary impact?*

P. Vogt, C. Bernero, L. Kovacs, P. Taylor, *Structure and plate tectonic evolution of the marine Arctic as revealed by aeromagnetics.*

W. W. Hay, *Sedimentological and geochemical trends resulting from the breakup of Pangaea.*

W. H. Berger, E. Vincent, *Chemostratigraphy and biostratigraphic correlation exercises in systemic stratigraphy.*